Glacial meltwater and sea ice meltwater in the Prydz Bay, Antarctica

CAI Pinghe (蔡平河)[1], HUANG Yipu (黄奕普)[1], CHEN Min (陈 敏)[1], LIU Guangshan (刘广山)[1], QIU Yusheng (邱雨生)[1], CHEN Xingbao (陈性保)[1], JIN Deqiu (金德秋)[2] & ZHOU Xihuang (周锡煌)[2]

1. Department of Oceanography, Xiamen University, Xiamen 361005, China;
2. Department of Chemistry, Peking University, Beijing 100871, China
Correspondence should be addressed to Cai Pinghe (email: caiph@jingxian.xmu.edu.cn)

Received April 5, 2002

Abstract Measurements of d D and salinity were carried out in the Prydz Bay during two Antarctic cruises, the 13th and the 14th Chinese National Antarctic Research expeditions (CHINARE). Mass balance calculations based on d D and salinity showed that during the 13th CHINARE cruise, percentages of glacial meltwater and sea ice meltwater in the study region ranged from 0% to 3.82% and from –3.19% to 4.78%, respectively. Meanwhile, the percentages were 1.53%—3.98% and –3.80%—4.52% during the 14th CHINARE cruise. We depicted plots showing the horizontal distributions of glacial meltwater and sea ice meltwater, and found a footprint of Circumpolar Deep Water (CDW), which may suggest a strong upwelling in this regime. We also noticed a butterfly-like image in the plot, which resulted from two adjacent water masses. It is interesting to note that the butterfly-like image deflected anticlockwise with depth. We suggested that the cause of the deflection could be due to Ekman effect. Depth profiles of glacial meltwater within the Prydz Bay were fundamentally uniform, revealing that inflow of glacial meltwater to the basin was a slower process with respect to the vertical mixing in the water column. Nevertheless, percentage of sea ice meltwater decreased steadily with depth, presumably due to the effect of seasonal cycle of sea ice production.

Keywords: glacial meltwater, sea ice meltwater, d D, Antarctica, Prydz Bay.

It has been well known by oceanographers that the World Ocean Circulation originates in North Atlantic near the Greenland, where in wintertime the cooled surface water descends to form North Atlantic Deep Waters (NADW). The NADW, when passing the Antarctica, receives the Antarctic Bottom Water (AABW). As the Antarctic Bottom Water has characteristics of low temperature and high components of glacial meltwater, it considerably influences the ocean heat budget via the World Ocean Circulation. In recent years, the mass balance of Antarctic Ice Cap has drawn substantial interest from numerous scientists, because of its critical role in the variation of sea level. Unfortunately, the term melting velocity of Antarctic Ice Cap in the mass balance calculation remains a puzzling issue. Nevertheless, if one has obtained some knowledge of the glacial meltwater content in the Antarctic margins, the melting velocity of Antarctic Ice Cap can

be deduced when combined with the outflow measurements of seawater in these regimes.

It is difficult, however, to estimate the percentages of glacial meltwater and sea ice meltwater if only CTD data are available. This is primarily because water masses at high latitudes generally comprise at least three components. Accordingly, percentage calculations require at least three conservative parameters for the mass balance equations. Besides mass and salinity, the isotopic composition defined as d D(d^2H) and d^{18}O is also a conservative property of seawater. The hydrogen and oxygen isotope composition in seawater shows only a slight variation except at high latitudes or near those coastal margins where there is significant input or removal of fresh water. Due to the isotopic fractionation processes that occur during evaporation, condensation and sea ice freezing, precipitation is generally depleted in the heavier isotopes of hydrogen and oxygen, whereas sea ice is heavier isotopes-rich. Moreover, the fractionation processes are temperature dependent. Hence, precipitation at higher latitudes and higher elevations shows a progressively lower d D and d^{18}O values. As such, one would expect that seawater, glacial meltwater and sea ice meltwater in these regimes differ considerably in isotopic composition. The advantage has been taken by researchers to determine distinct components of water masses in higher-latitude regions when combined with measurements of salinity[1−5]. Successful applications of d D and d^{18}O include deduction of ice melt inputs to coastal waters and determination of source waters in the Arctic region. Few studies, however, have been undertaken in the Antarctic margins before this work.

1 Sample collection

The Prydz Bay is one of the three major Antarctic coastal seas (the other two are Weddell Sea and Ross Sea). It locates in the southern Indian Ocean sector. Water depth in the basin is around 500—600 m, with a maximum of more than 800 m. During the 13th (from November 1996 to April 1997) and the 14th (from November 1997 to April 1998) CHINARE cruises, seawater samples were collected at 30 stations in the Prydz Bay. The occupied domain was from 65°S to 69°20′S and 70°E to 78°E. Sampling locations are shown in fig. 1. Seawater samples were taken at selected depths using Go-Flo samplers attached to a CTD system. We also collected glacial ice and sea ice samples in the study region. After collection, the ice samples were set under near 0℃ circumstance and melt slowly. The glacial meltwater, sea ice meltwater as well as seawater samples were stored in 50-mL PVC bottles. Onshore, hydrogen isotope

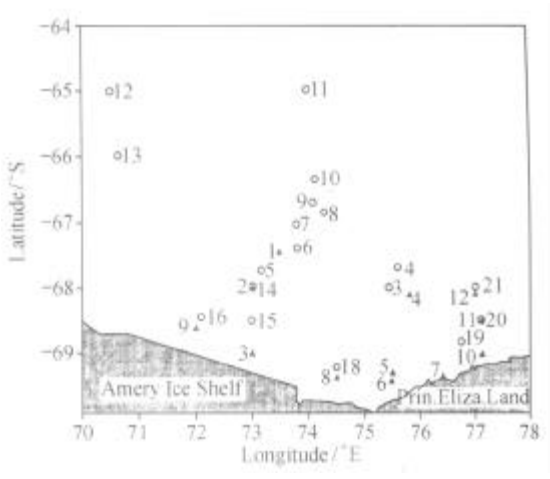

Fig. 1. Locations of the sampling stations in the Prydz Bay, Antarctica, from the 13th (open circles) and the 14th (closed triangles) CHINARE cruises.

composition of the samples was determined with a mass spectrometer in the Department of Chemistry, Peking University.

2 Hydrogen isotope analysis

Analytical procedure involved the reduction of water with zinc and the isotopic analysis of hydrogen gas[6].

2.1 Reduction of water

The reagent used is Analar zinc shot (BDH Ltd., England). The zinc shot was washed successively in diluted nitric acid, tap water, deionized water and acetone, then dried, outgassed and stored in dry nitrogen. Approximately 0.2 g of the zinc shot was put into a reaction tube (Ø8×160 mm). The tube was sealed and attached to a suitable vacuum line. The vessel was evacuated to <0.5 Pa and outgassed for 2 h by warming to about 200℃ using a hot air gun. Having been cooled, the tube was filled with dry nitrogen. 10 μL of water sample was introduced to the bottom of the tube using a syringe. Liquid nitrogen was used to freeze the water sample. The evacuated tube containing zinc shot and water sample was put into a heating block at 450℃. After about 2 h, the tube was attached to the mass spectrometer inlet system for isotopic analysis without any further cleanup of the gas.

2.2 Isotopic analysis

The isotopic composition of the gas is measured with a mass spectrometer VG SIRA-24. The isotopic composition of the water sample is expressed as d D, which is the fractional difference between ratios of the sample and a standard reference:

$$d\,\mathrm{D}\ (‰) = \left(\frac{R_{3/2\ \mathrm{sample}}}{R_{3/2\ \mathrm{reference}}} - 1 \right) \times 1000,$$

where $R_{3/2}$ is the isotopic abundance ratio of mass 3 to 2.

The samples were run and measured against a reference gas. The contribution from H^{3+} to the HD ion beam has been corrected automatically. To get the d D values against VSMOW, national standard substances GBW 04401 (d D = −0.4‰) and GBW 04404 (d D = −428.3‰) were measured simultaneously with samples. Duplicate analyses were conducted for all samples. Results indicated that the precision was generally within 1‰.

3 Results and discussion

3.1 Percentage calculations of glacial meltwater and sea ice meltwater

Salinity and d D in seawater from the study region are given in table 1. As shown in table 1, d D varies between − 6.5‰ and 0.5‰. Since Circumpolar Deep Water (CDW) is the only water mass that intrudes southward into the Antarctic margins[7], we thus speculate that all water masses

Table 1 Salinity, δD, F_{CDW}, F_{MW} and F_{SIM} in the seawater

Sta./Location/Time	Depth/m	δD ± σ (‰)	S	F_{CDW}(%)	F_{MW}(%)	F_{SIM}(%)
13-3#	0	−4.4 ± 0.2	33.725	97.21	2.90	−0.11
	25	−4.8 ±0.3	34.117	98.61	3.00	−1.61
68° 01′S, 75° 27′E	50	−4.1 ± 0.5	34.289	99.11	2.53	−1.64
	100	−4.6 ± 0.1	34.420	99.62	2.78	−2.40
1997-01-10	150	−4.3 ± 0.1	34.462	99.73	2.59	−2.32
	200	−4.0 ± 0.4	34.479	99.75	2.41	−2.16
	300	−3.6 ± 0.3	34.504	99.78	2.17	−1.95
	450	−4.7 ± 0.1	34.540	100.05	2.80	−2.85
13-4#	0	−4.0 ± 0.4	33.438	96.17	2.77	1.06
	25	−3.9 ± 0.2	34.051	98.27	2.50	−0.77
67°43′S, 75°38′E	50	−3.8 ± 0.4	34.297	99.10	2.36	−1.46
	100	−4.6 ± 0.1	34.368	99.44	2.80	−2.24
1997-01-10	150	−3.2 ± 0.2	34.436	99.50	1.96	−1.46
	200	−2.6 ± 0.1	34.505	99.66	1.58	−1.25
	300	−2.9 ± 0.4	34.514	99.73	1.76	−1.49
	350	−3.4 ± 0.1	34.522	99.82	2.05	−1.87
13-5#	0	−3.6 ± 0.4	34.034	98.17	2.33	−0.50
	25	−4.8 ± 0.4	34.205	98.91	2.97	−1.88
67° 44′S, 73° 10′E	50	−3.9 ± 0.3	34.319	99.19	2.41	−1.59
	100	−2.7 ± 0.1	34.489	99.62	1.65	−1.27
1997-01-10	150	−2.9 ± 0.1	34.501	99.68	1.76	−1.45
	200	−3.0 ± 0.2	34.500	99.69	1.82	−1.51
	300	−3.2 ± 0.3	34.512	99.76	1.93	−1.69
	500	−4.2 ± 0.3	34.579	100.12	2.49	−2.61
13-6#	0	−3.8 ± 0.1	33.522	96.44	2.62	0.94
	25	−4.4 ± 0.2	34.208	98.87	2.74	−1.61
67°02′S, 73°48′E	50	−3.5 ± 0.1	34.348	99.24	2.16	−1.40
	100	−3.2 ± 0.1	34.406	99.40	1.97	−1.37
1997-01-11	200	−4.8 ± 0.1	34.535	100.04	2.86	−2.90
	250	−4.6 ± 0.2	34.506	99.92	2.75	−2.67
	500	−4.8 ± 0.5	34.628	100.36	2.83	−3.19
13-7#	0	−3.5 ± 0.5	32.562	93.10	2.77	4.13
	25	−4.1 ± 0.6	34.056	98.31	2.61	−0.92
67°02′S, 73°48′E	50	−4.0 ± 0.5	34.157	98.64	2.52	−1.16
	100	−4.0 ± 0.3	34.262	99.00	2.49	−1.49
1997-01-11	150	−4.9 ± 0.6	34.340	99.39	2.98	−2.37
	200	−5.2 ± 0.3	34.371	99.53	3.15	−2.68
	300	−4.6 ± 0.2	34.459	99.76	2.77	−2.53
	400	−4.2 ± 0.4	34.538	99.98	2.51	−2.49
13-8#	0	−4.2 ± 0.5	33.748	97.26	2.78	−0.04
	25	−6.1 ± 0.3	33.957	98.22	3.82	−2.04
66°52′S, 74°19′E	50	−5.5 ± 0.2	34.110	98.67	3.41	−2.09
	100	−4.0 ± 0.2	34.294	99.11	2.47	−1.59
1997-01-12	150	−3.5 ± 0.2	34.331	99.18	2.17	−1.35
	200	−3.8 ± 0.1	34.353	99.29	2.34	−1.63
13-8#	300	−2.3 ± 0.4	34.481	99.54	1.42	−0.96
	500	−2.3 ± 0.0	34.579	99.88	1.38	−1.26
	800	−1.4 ± 0.1	34.673	100.09	0.83	−0.91
	1000	−1.5 ± 0.4	34.672	100.09	0.89	−0.98
	1200	0.0 ± 0.1	34.674	99.91	0.01	0.08
13-9#	0	−2.3 ± 0.3	33.019	94.52	1.92	3.57
	25	−2.7 ± 0.3	33.990	97.90	1.82	0.28
66° 41′S, 74° 07′E	50	−2.7 ± 0.3	34.172	98.53	1.76	−0.29
	100	−3.3 ± 0.2	34.254	98.89	2.08	−0.97
1997-01-14	150	−3.3 ± 0.3	34.296	99.03	2.06	−1.10
	200	−3.1 ± 0.1	34.353	99.20	1.93	−1.13
	500	−1.4 ± 0.4	34.616	99.89	0.85	−0.74
	800	−1.3 ± 0.1	34.673	100.07	0.77	−0.84
	1000	−0.4 ± 0.1	34.674	99.96	0.24	−0.20
	1500	−0.7 ± 0.4	34.669	99.98	0.42	−0.40
13-10#	0	−2.2 ± 0.2	32.651	93.24	1.98	4.78
	25	−2.6 ± 0.4	34.044	98.08	1.74	0.18
66° 22′S, 74° 09′E	50	−2.5 ± 0.4	34.196	98.59	1.63	−0.22
	100	−1.9 ± 0.4	34.256	98.72	1.26	0.02
1997-01-14	150	−2.7 ± 0.1	34.306	98.99	1.71	−0.70
	200	−1.6 ± 0.4	34.343	98.98	1.06	−0.03
	300	−1.5 ± 0.1	34.481	99.44	0.95	−0.39
	500	−0.7 ± 0.1	34.628	99.84	0.43	−0.27
	850	0.1 ± 0.1	34.682	99.93	-0.05	0.13
13-11#	0	−4.5 ± 0.4	32.847	94.21	3.26	2.53
	25	−4.9 ± 0.2	33.704	97.20	3.20	−0.40
64° 59′S, 73° 58′E	50	−4.3 ± 0.4	34.033	98.26	2.74	−0.99
	100	−3.8 ± 0.2	34.298	99.10	2.36	−1.46
1997-01-15	150	−4.3 ± 0.2	34.387	99.47	2.62	−2.09
	200	−3.4 ± 0.2	34.606	100.11	2.02	−2.13
	300	−2.7 ± 0.4	34.677	100.26	1.58	−1.85
	400	−2.3 ± 0.4	34.692	100.26	1.35	−1.61
13-12#	0	−4.9 ± 0.5	33.761	97.40	3.18	−0.58
	25	−4.3 ± 0.4	33.771	97.36	2.83	−0.18
65° 02′S, 70° 30′E	50	−4.7 ± 0.2	34.095	98.52	2.95	−1.47
	100	−4.4 ± 0.6	34.385	99.48	2.68	−2.15
1997-01-16	150	−4.0 ± 0.3	34.452	99.66	2.42	−2.08
	200	−2.9 ± 0.1	34.510	99.72	1.76	−1.47
	300	−2.1 ± 0.3	34.622	100.00	1.25	−1.25
	500	−1.6 ± 0.1	34.691	100.17	0.94	−1.11
	1500	−0.2 ± 0.5	34.679	99.95	0.12	−0.08
	2500	0.0 ± 0.1	34.668	99.89	0.01	0.10
13-13#	0	−3.5 ± 0.2	33.199	95.29	2.55	2.16
	25	−3.3 ± 0.3	33.737	97.11	2.26	0.63
	50	−3.6 ± 0.3	34.088	98.36	2.31	−0.67

(To be continued on the next page)

(*Continued*)

Sta./Location/Time	Depth/m	$\delta D \pm \sigma$ (‰)	S	F_{CDW}(%)	F_{MW}(%)	F_{SIM}(%)
13-13#	100	−2.8 ± 0.2	34.333	99.10	1.76	−0.86
	150	−2.7 ± 0.1	34.465	99.54	1.66	−1.19
66°02′S, 70°40′E	200	−2.5 ± 0.3	34.590	99.94	1.50	−1.44
	300	−2.9 ± 0.2	34.671	100.27	1.70	−1.97
1997-01-16	500	−2.1 ± 0.1	34.690	100.23	1.23	−1.46
	1500	−1.5 ± 0.2	34.671	100.09	0.89	−0.98
	2300	0.5 ± 0.2	34.667	99.82	0.00	0.18
13-14#	0	−3.8 ± 0.3	33.230	95.43	2.72	1.85
	25	−4.0 ± 0.4	33.941	97.90	2.59	−0.50
67°58′S, 72°59′E	50	−3.5 ± 0.5	34.259	98.93	2.19	−1.12
	100	−2.6 ± 0.4	34.399	99.30	1.62	−0.92
1997-01-22	150	−2.7 ± 0.3	34.478	99.58	1.65	−1.23
	200	−2.5 ± 0.1	34.504	99.64	1.53	−1.17
	300	−2.2 ± 0.3	34.535	99.71	1.34	−1.05
	550	−2.3 ± 0.1	34.622	100.02	1.37	−1.39
13-15#	0	−3.9 ± 0.3	34.033	98.20	2.50	−0.71
	25	−3.7 ± 0.1	34.360	99.30	2.28	−1.58
68′30′S, 72°59′E	50	−4.6 ± 0.1	34.418	99.62	2.78	−2.40
	100	−5.1 ± 0.3	34.456	99.81	3.06	−2.87
1997-01-22	150	−4.9 ± 0.4	34.475	99.85	2.94	−2.79
	200	−4.0 ± 0.4	34.487	99.78	2.41	−2.19
	300	−4.6 ± 0.1	34.502	99.90	2.75	−2.66
	500	−4.5 ± 0.1	34.515	99.94	2.69	−2.63
13-16#	0	−3.1 ± 0.1	34.151	98.51	2.00	−0.51
	25	−3.0 ± 0.1	34.272	98.91	1.90	−0.81
68°27′S, 72°04′E	50	−4.0 ± 0.1	34.433	99.59	2.43	−2.02
	100	−3.9 ± 0.1	34.492	99.78	2.35	−2.13
1997-01-22	150	−4.0 ± 0.1	34.499	99.82	2.40	−2.22
	200	−4.2 ± 0.2	34.504	99.86	2.52	−2.38
	300	−4.3 ± 0.4	34.516	99.91	2.57	−2.49
	450	−4.5 ± 0.5	34.532	99.99	2.69	−2.68
13-18#	0	−4.4 ± 0.2	34.131	98.60	2.76	−1.37
	25	−4.5 ± 0.2	34.126	98.60	2.82	−1.42
69°10′S, 74°30′E	50	−4.3 ± 0.6	34.373	99.42	2.62	−2.05
	100	−4.2 ± 0.1	34.456	99.70	2.54	−2.23
1997-01-23	150	−4.7 ± 0.1	34.465	99.79	2.83	−2.62
	200	−4.0 ± 0.2	34.469	99.71	2.41	−2.13
	300	−3.5 ± 0.5	34.485	99.71	2.12	−1.82
	500	−3.6 ± 0.2	34.502	99.78	2.17	−1.95
	750	−3.1 ± 0.2	34.520	99.78	1.87	−1.65
13-19#	0	−3.1 ± 0.5	33.952	97.82	2.07	0.11
	25	−1.9 ± 0.2	34.149	98.35	1.30	0.35
68°50′S, 76°44′E	50	−2.4 ± 0.4	34.338	99.06	1.52	−0.59
	100	−2.2 ± 0.4	34.398	99.24	1.39	−0.63
1997-01-23	150	−2.0 ± 0.1	34.453	99.41	1.25	−0.66
13-19#	200	−2.0 ± 0.3	34.448	99.39	1.25	−0.64
	300	−2.5 ± 0.1	34.472	99.53	1.54	−1.07
	500	−2.6 ± 0.6	34.500	99.64	1.59	−1.23
	700	−2.5 ± 0.4	34.516	99.69	1.52	−1.21
13-20#	0	−2.3 ± 0.1	33.943	97.69	1.60	0.71
	25	−2.5 ± 0.5	34.080	98.19	1.67	0.14
68° 31′S, 77° 03′E	50	−2.4 ± 0.1	34.297	98.92	1.54	−0.46
	100	−2.6 ± 0.1	34.372	99.20	1.63	−0.83
1997-01-23	150	−2.7 ± 0.1	34.435	99.43	1.67	−1.10
	200	−3.2 ± 0.1	34.459	99.58	1.95	−1.53
	300	−3.4 ± 0.1	34.483	99.69	2.06	−1.75
	600	−2.8 ± 0.2	34.535	99.79	1.69	−1.48
13-21#	0	−4.2 ± 0.1	33.438	96.20	2.88	0.92
	25	−2.6 ± 0.4	33.918	97.64	1.78	0.57
68° 00′S, 77° 01′E	50	−3.2 ± 0.2	34.292	99.01	2.01	−1.01
	100	−2.7 ± 0.1	34.407	99.34	1.68	−1.01
1997-01-23	150	−3.0 ± 0.1	34.464	99.57	1.83	−1.40
	390	−3.6 ± 0.2	34.523	99.85	2.16	−2.01
14-1#	0	−3.3 ± 0.2	32.826	93.98	2.56	3.45
	25	−3.0 ± 0.4	32.942	94.34	2.35	3.31
67° 27′S, 73° 32′E	50	−3.0 ± 0.3	34.235	98.78	1.91	−0.69
	100	−2.6 ± 0.4	34.345	99.11	1.64	−0.75
1998-02-15	150	−2.9 ± 0.3	34.429	99.44	1.79	−1.22
	200	−2.5 ± 0.3	34.494	99.61	1.53	−1.14
	300	−3.5 ± 0.1	34.493	99.73	2.11	−1.85
	400	−3.5 ± 0.4	34.505	99.77	2.11	−1.89
14-2#	0	−3.3 ± 0.1	32.692	93.52	2.61	3.87
	25	−4.0 ± 0.4	34.065	98.33	2.55	−0.88
68° 00′S, 73° 00′E	50	−4.1 ± 0.1	34.286	99.10	2.54	−1.63
	100	−3.9 ± 0.5	34.415	99.52	2.37	−1.89
1998-02-01	150	−3.9 ± 0.1	34.428	99.56	2.37	−1.93
	200	−4.0 ± 0.2	34.433	99.59	2.43	−2.02
	300	−4.1 ± 0.2	34.411	99.53	2.49	−2.02
	500	−4.5 ± 0.5	34.462	99.75	2.71	−2.46
	600	−4.9 ± 0.3	34.527	100.03	2.92	−2.95
14-3#	0	−4.8 ± 0.4	32.162	91.89	3.67	4.44
	25	−4.9 ± 0.3	33.922	97.95	3.13	−1.08
68° 40′S, 73° 03′E	50	−5.0 ± 0.2	34.255	99.11	3.07	−2.18
	100	−4.5 ± 0.3	34.335	99.32	2.75	−2.07
1998-01-30	150	−4.4 ± 0.1	34.367	99.42	2.68	−2.10
	200	−4.8 ± 0.6	34.382	99.52	2.91	−2.43
	300	−5.1 ± 0.1	34.420	99.69	3.07	−2.76
	500	−5.3 ± 0.6	34.439	99.78	3.18	−2.96
	750	−4.9 ± 0.5	34.494	99.92	2.93	−2.85
14-4#	0	−3.2 ± 0.5	32.502	92.86	2.62	4.53

(*To be continued on the next page*)

(*Continued*)

Sta./Location/Time	Depth/m	$\delta D \pm \sigma$ (‰)	S	F_{CDW}(%)	F_{MW}(%)	F_{SIM}(%)
14-4#	25	−3.1 ± 0.1	32.908	94.24	2.42	3.34
	50	−3.6 ± 0.2	34.171	98.64	2.28	−0.92
68°04′S, 75°50′E	100	−3.5 ± 0.3	34.352	99.25	2.16	−1.41
	150	−3.6 ± 0.1	34.386	99.38	2.21	−1.59
1998-02-01	200	−3.3 ± 0.3	34.402	99.40	2.03	−1.42
	300	−3.7 ± 0.5	34.435	99.56	2.25	−1.81
	440	−3.8 ± 0.4	34.460	99.66	2.30	−1.96
14-5#	0	−3.3 ± 0.2	33.727	97.08	2.26	0.66
	15	−3.5 ± 0.5	33.766	97.24	2.36	0.40
69° 08′S, 75° 30′E	25	−3.8 ± 0.2	34.061	98.29	2.44	−0.72
	50	−3.7 ± 0.3	34.207	98.78	2.33	−1.11
1998-01-23	100	−3.5 ± 0.3	34.366	99.30	2.16	−1.46
	200	−3.6 ± 0.2	34.399	99.42	2.21	−1.63
	580	−4.1 ± 0.1	34.437	99.62	2.48	−2.10
	680	−4.3 ± 0.1	34.453	99.70	2.60	−2.29
14-6#	0	−3.8 ± 0.2	33.151	95.16	2.75	2.09
	15	−4.0 ± 0.1	33.211	95.39	2.84	1.76
69°21′S, 75°30′E	25	−3.7 ± 0.1	33.270	95.56	2.65	1.79
	50	−3.9 ± 0.2	33.700	97.06	2.62	0.32
1998-02-17	100	−3.5 ± 0.1	34.233	98.84	2.20	−1.04
	150	−3.9 ± 0.4	34.322	99.20	2.41	−1.60
	220	−4.0 ± 0.4	34.397	99.47	2.44	−1.91
14-7#	0	−5.5 ± 0.3	33.015	94.91	3.79	1.30
	15	−5.8 ± 0.1	32.935	94.67	3.99	1.34
69°21′S, 76°25′E	25	−5.8 ± 0.4	32.953	94.74	3.98	1.28
	50	−5.5 ± 0.4	33.746	97.42	3.54	−0.96
1998-02-18	100	−5.5 ± 0.2	34.129	98.74	3.41	−2.14
	150	−5.3 ± 0.4	34.273	99.21	3.24	−2.45
	200	−5.6 ± 0.4	34.325	99.42	3.40	−2.82
	300	−5.6 ± 0.4	34.403	99.69	3.37	−3.06
	400	−5.9 ± 0.6	34.443	99.87	3.53	−3.40
	550	−5.9 ± 0.3	34.467	99.95	3.53	−3.47
14-8#	0	−4.4 ± 0.6	33.730	97.23	2.90	−0.13
	25	−4.3 ± 0.6	33.938	97.93	2.77	−0.70
69°21′S, 74°30′E	50	−4.4 ± 0.5	34.184	98.79	2.75	−1.53
	100	−4.4 ± 0.4	34.293	99.16	2.71	−1.87
1998-01-30	150	−4.3 ± 0.6	34.354	99.36	2.63	−1.99
	200	−4.8 ± 0.4	34.368	99.47	2.92	−2.39
	300	−4.4 ± 0.2	34.397	99.52	2.67	−2.19
	500	−4.6 ± 0.1	34.419	99.62	2.78	−2.40
	600	−5.7 ± 0.6	34.432	99.80	3.42	−3.22
	700	−6.2 ± 0.4	34.453	99.94	3.71	−3.64
14-9#	0	−4.1 ± 0.1	33.263	95.59	2.88	1.53
	25	−4.7 ± 0.5	34.109	98.57	2.95	−1.51
	50	−5.5 ± 0.5	34.265	99.20	3.36	−2.57
14-9#	100	−5.6 ± 0.2	34.336	99.46	3.39	−2.86
68° 35′S, 72°00′E	150	−6.0 ± 0.4	34.342	99.53	3.63	−3.16
	200	−6.0 ± 0.1	34.364	99.61	3.62	−3.23
1998-02-01	300	−6.4 ± 0.1	34.401	99.79	3.84	−3.63
	400	−6.5 ± 0.2	34.434	99.91	3.89	−3.80
14-10#	0	−3.6 ± 0.1	33.118	95.02	2.64	2.34
	25	−3.2 ± 0.1	33.735	97.09	2.20	0.71
68°58′S, 77°05′E	50	−4.2 ± 0.4	34.051	98.30	2.67	−0.98
	100	−4.5 ± 0.2	34.267	99.08	2.78	−1.86
1998-02-01	150	−4.7 ± 0.2	34.304	99.24	2.88	−2.12
	200	−4.5 ± 0.3	34.340	99.34	2.75	−2.09
	300	−4.4 ± 0.1	34.389	99.49	2.68	−2.17
	500	−4.6 ± 0.2	34.423	99.63	2.78	−2.41
	600	−5.5 ± 0.4	34.438	99.80	3.30	−3.10
14-11#	0	−4.3 ± 0.4	33.376	96.00	2.96	1.04
	25	−5.4 ± 0.1	33.412	96.26	3.59	0.15
68°30′S, 77°05′E	50	−5.5 ± 0.4	33.995	98.28	3.45	−1.73
	100	−5.8 ± 0.2	34.273	99.27	3.53	−2.80
1998-02-01	150	−5.5 ± 0.2	34.324	99.41	3.34	−2.75
	200	−5.3 ± 0.5	34.355	99.49	3.21	−2.70
	300	−5.0 ± 0.3	34.385	99.55	3.03	−2.58
	450	−5.4 ± 0.4	34.411	99.69	3.25	−2.95
14-12#	0	−4.0 ± 0.2	32.895	94.31	2.95	2.74
	25	−4.3 ± 0.3	33.229	95.49	3.01	1.49
68°04′S, 77°00′E	50	−4.2 ± 0.6	34.212	98.86	2.62	−1.48
	100	−4.9 ± 0.4	34.313	99.29	2.99	−2.29
1998-02-01	150	−4.6 ± 0.2	34.356	99.40	2.80	−2.21
	200	−4.5 ± 0.1	34.382	99.48	2.74	−2.22
	300	−4.9 ± 0.6	34.402	99.60	2.96	−2.56
	450	−4.5 ± 0.5	34.466	99.77	2.71	−2.48

there originate chiefly from the interaction of Circumpolar Deep Water, glaciers and sea ice. By applying mass balance equations, percentages of seawater components in the Prydz Bay can be quantified by

$$F_{CDW} + F_{MW} + F_{SIM} = 1, \quad (1)$$

$$F_{CDW} \cdot S_{CDW} + F_{MW} \cdot S_{MW} + F_{SIM} \cdot S_{SIM} = S \quad (2)$$

and

$$F_{CDW} \cdot d\,D_{CDW} + F_{MW} \cdot d\,D_{MW} + F_{SIM} \cdot d\,D_{SIM} = d\,D, \quad (3)$$

where F denotes percentage, S is salinity, d D is hydrogen isotope composition. The subscriptions CDW, MW and SIM are Circumpolar Deep Water, glacial meltwater and sea ice meltwater, respectively. Measurements showed that d D values in glacial meltwater from the two CHINARE cruises were –146.7‰ ± 0.4‰ and –155.1‰ ± 0.6‰, and the mean was –151.0‰ ± 0.4‰. During the 15th CHINARE cruise, Liu et al.[8] collected numerous snow samples and fresh lake water samples. Isotopic analysis showed that mean dDs of the snow and lake waters were –159.6‰ and –153.7‰, in close agreement with our results. Generally, precipitation is characterized by very low salinity, and therefore, it was assumed to have a salinity of zero in this study. As mentioned above, sea ice is rich in heavier isotope ^{2}H because of isotopic fractionation processes that occur during sea ice freezing. In this study, we also determined the hydrogen isotope composition in sea ice meltwater and found that the d Ds were 16.7‰ ± 0.1‰ and 16.4‰ ± 0.5‰, with an average of 16.6‰ ± 0.3‰. Lenmann and Siegenthaler[9] have demonstrated that the equilibrium hydrogen isotope fractionation factor between ice and water is 1.0204; that is, d D in sea ice is 20.4‰ heavier than that in underlying water. As shown in table 1, surface d D in the study region was around – 4.0‰. According to Lenmann and Siegenthaler[9], dD = 16.4‰ in sea ice would be expected under equilibrium fractionation, which agrees very well with our measurement. Sea ice salinity has been determined to be 6.2 by Macdonald et al.[5], i.e. S_{SIM} = 6.2. Circumpolar Deep Water (CDW) is by far the most abundant water mass in the region, with core salinity of around 34.70[10]. Our measurement suggested that its d D was approximately 0.0 ‰, comparable to the results obtained by Zeng et al.[1)] and Liu et al.[2)] from the 15th CHINARE cruise.

Substituting the typical S and d D to eqs. (1)—(3), we get

$$F_{CDW} + F_{MW} + F_{SIM} = 1, \quad (4)$$

$$34.70\,F_{CDW} + 6.2\,F_{SIM} = S \quad (5)$$

and

$$-151F_{MW} + 16.6\,F_{SIM} = d\,D. \quad (6)$$

Based on the above equations, F_{CDW}, F_{MW} and F_{SIM} were calculated. Results have been listed in table 1. As shown in table 1, F_{MW} and F_{SIM} in the study region ranged from 0.0% to 3.82% and from –3.19% to 4.78% during the 13th CHINARE cruise, whereas during the 14th CHINARE

1) Zeng, X. Z., Yin, M. D., Zeng, W. Y. et al., Distribution features of ^{18}O and NO in the Prydz Bay and its implications for physical oceanography (submitted to Science in China, Ser. D), 2002.

2) Liu, G. S., Huang, Y. P., Chen, M. et al., Water mass ädD in the Prydz Bay, Antarctica (submitted to Journal of Xiamen University (Natural Science)), 2002.

cruise, the percentages were 1.53%—3.98% and –3.80%—4.52%, respectively. Note that F_{SIM} could be either positive or negative. For example, surface F_{CDW}, F_{MW} and F_{SIM} at station 2 from the 14th CHINARE cruise were 93.52%, 2.61% and 3.87%, meaning that 100 g of the seawater was the mixture of 93.52 g of Circumpolar Deep Water, 2.61 g of glacial meltwater and 3.87 g of sea ice meltwater. Meanwhile, at the same station, F_{CDW}, F_{MW} and F_{SIM} at 200 m were 99.59%, 2.43% and –2.02%. The implication is that 100 g of the seawater was produced by the mixture of 99.59 g of Circumpolar Deep Water and 2.43 g of glacial meltwater, which subsequently released 2.02 g of sea ice by freezing.

3.2 Horizontal distributions of glacial meltwater and sea ice meltwater

Plots showing horizontal distributions of F_{MW} and F_{SIM} at 0, 25, 50, 100, 150, 200, 300 m from the 13th CHINARE cruise were depicted. Here, for the ease of interpretation, only F_{MW} plots at 50 and 200 m, and F_{SIM} plots at 100 and 200 m are shown in figs. 2 and 3. Other plots showed

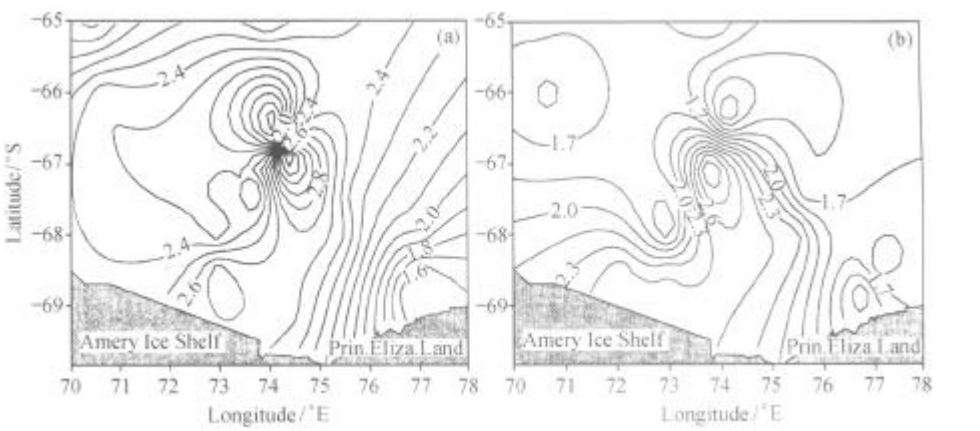

Fig. 2. Horizontal distributions of F_{MW} (%) at 50 m (a) and 200 m (b) from the 13th CHINARE cruise.

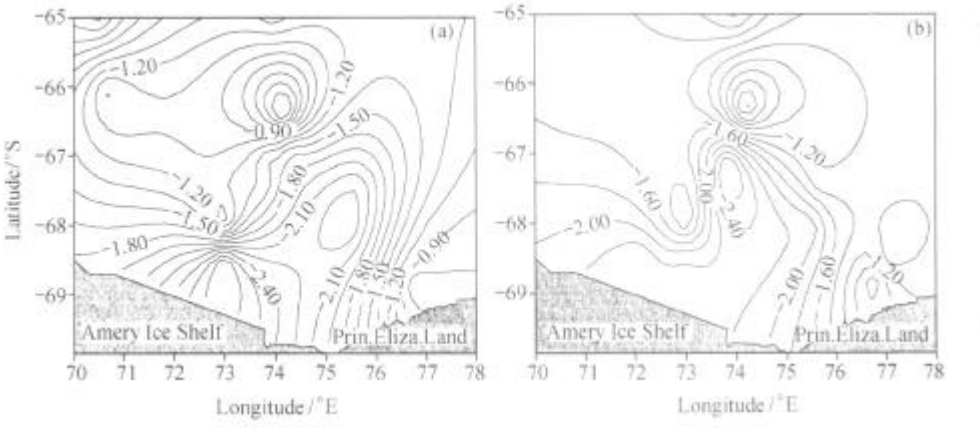

Fig. 3. Horizontal distributions of F_{SIM} (%) at 100 m (a) and 200 m (b) from the 13th CHINARE cruise.

similar distribution patterns. In figs. 2 and 3, two water masses were evident: one was centered around 66.5°S, 74°E and could be identified by its low F_{MW} and high F_{SIM}. The other, which was characterized by high F_{MW} and low F_{SIM}, was centered around 67°S, 74°E. Interestingly, the two water masses formed a butterfly-like image. Judging from the salinity and d D, we suggest that the water mass around 66.5°S, 74°E is a footprint of Circumpolar Deep Water, and the other is the continental shelf water as identified by Smith et al.[10]. Since the Prydz Bay is a semi-enclosed basin, water exchange with open oceans should be restricted. Thus, one would expect a longer water residence time within the basin, which allowed significant accumulations of glacial meltwater and saline water released by ice freezing. Accordingly, as shown above, the continental shelf water was identified by high contents of glacial meltwater and saline water (i.e. high F_{MW} and low F_{SIM}). In the oceanic domain, it is very likely that water residence time is considerably shorter than that within the basin due to the strong upwelling of Circumpolar Deep Water. The shorter residence time may therefore greatly constrain the accumulations of glacial meltwater and saline water. As such, one would expect that low F_{MW} and high F_{SIM} were typical of open waters.

It is worthwhile to note an interesting phenomenon in figs. 2 and 3. The butterfly-like images in figs. 2(a) and 3(a) are northeast oriented, while in figs. 2(b) and 3(b) the images are northwest oriented, as a butterfly rotates by 90 degrees while flying. We ascribed the phenomenon to the Ekman effect. As we know that the region is dominated by strong easterly, a wind-driven current with its direction deflecting by 45 degrees to the left-hand side of the wind direction would occur at the sea surface because of the Ekman effect[11]. Moreover, in the Southern Hemisphere the current would further deflect anticlockwise with increasing depth. Accordingly, most contours in figs. 2(a) and 3(a) extend southwestward, whereas contours below 100 m mainly stretch southeastward (figs. 2(b) and 3(b)).

Fig. 4(a) and (b) exhibits the F_{MW} and F_{SIM} plots typical of the 14th CHINARE cruise. Al-

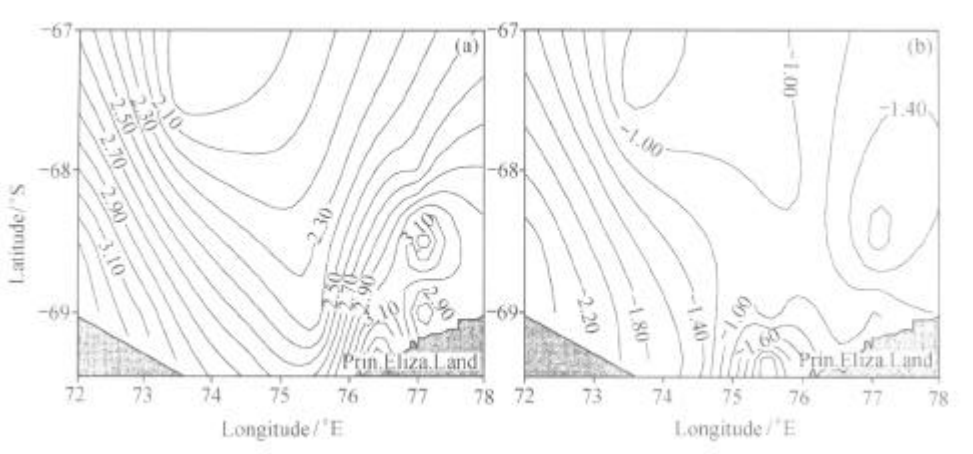

Fig. 4. Horizontal distributions of F_{MW} (a) and F_{SIM} (b) (%) at 50 m from the 14th CHINARE cruise.

though most stations of this cruise were located within the Prydz Bay, a landward increase trend in F_{MW} is still pronounced. Note that most contours in fig. 4(a) are nearly parallel to the edge of ice shelf. Additionally, F_{MW} increases steadily toward the ice shelf. This reveals that glacial meltwater in the basin may originate chiefly from the melting of ice shelf. By comparison of fig. 4, fig. 2 and fig. 3, one also sees the interannual variation in water composition, with F_{MW} and F_{SIM} from the 14th CHINARE cruise significantly higher than those from the 13th CHINARE cruise. One possible explanation is that the region was warmer during the 14th CHINARE cruise because of the prevailing El-Niño event. The higher temperature may intensify the melting of ice shelf and sea ice, and hence enhance the F_{MW} and F_{SIM} in seawater.

3.3 Vertical distributions of glacial meltwater and sea ice meltwater

Fig. 5(a) and (b) show the typical depth profiles of F_{MW} and F_{SIM} at station 2 from the 14th CHINARE cruise, and at station 12 from the 13th CHINARE cruise. As shown in fig. 5 and table 1, there are mainly two groups of depth profiles of glacial meltwater in the study region. Within the basin, most depth profiles of glacial meltwater were fundamentally uniform. Meanwhile, in the oceanic domain F_{MW} decreased steadily with depth. Nevertheless, F_{SIM} dropped progressively with depth within the basin, yet in the oceanic domain it decreased to a minimum, then increased slowly with depth. Again, we suggest that the patterns are related to water mixing process in the water column. As mentioned above, long residence time of the Prydz Bay water was assumed since the Prydz Bay is a semi-enclosed basin. In wintertime the descent of high-density saline water released by ice freezing would enhance vertical mixing in the water column. If the enhanced water mixing were a rapid process relative to the input of glacial meltwater, then one would expect a uniform depth profile of F_{MW} as depicted in fig. 5(a). In the oceanic domain, $F_{SIM} = 0$ and $F_{MW} = 0$ would be expected once the core of Circumpolar Deep Water is approached. Thus, as shown in fig. 5(b), F_{MW} decreased persistently to the depth where the core of Circumpolar Deep Water occurred. Note that F_{SIM} within the basin also showed a reduction with depth, which, we suspect, may be ascribed to the seasonal cycle of sea ice production. As the pack ice covered on the sea surface recedes in summertime, the sea ice meltwater, because of its low salinity and den-

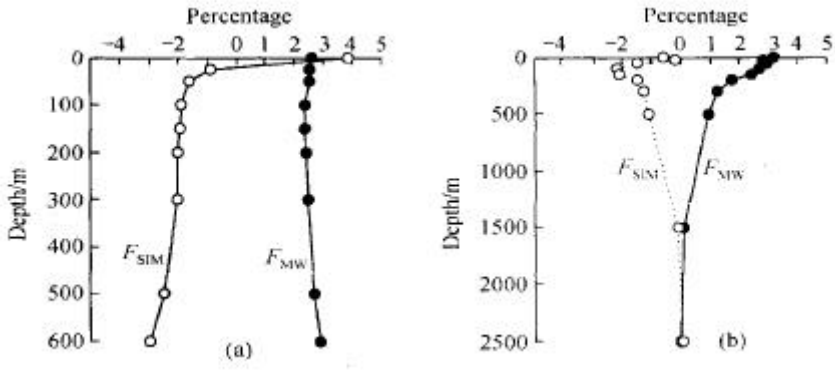

Fig. 5. Typical depth profiles of F_{MW} and F_{SIM} within the basin (a) and in oceanic domain (b).

sity, would reside mainly at the sea surface. In austral winter, high-density saline water released by ice freezing descends and accumulates in the lower water column. Both the effects of sea ice melting and saline water production would lead to the steady depth decrease in F_{SIM}. In the oceanic domain, F_{SIM} profiles in the upper water column were similar to those within the basin. In this case, with the approach of Circumpolar Deep Water, F_{SIM} increased to zero. Consequently, the overall depth profiles of F_{SIM} in open waters show an initial reduction, then a steady elevation with depth.

4 Conclusions

In this study, $\ddot{a}$D and salinity data were collected in the Prydz Bay, Antarctica, during the 13th and 14th CHINARE cruises. By applying mass balance equations, percentages of glacial meltwater and sea ice meltwater (F_{MW} and F_{SIM}) in seawater were estimated to be 0%—3.82% and –3.19%—4.78% for the 13th CHINARE cruise, and to be 1.53%—3.98% and –3.80%—4.52% for the 14th CHINARE cruise.

From the horizontal distributions of F_{MW} and F_{SIM}, we see a butterfly-like image resulting from two adjacent water masses. The water mass in the oceanic domain was characterized by low F_{MW} and high F_{SIM}, and was confirmed to be a footprint of Circumpolar Deep Water. Meanwhile, high F_{MW} and low F_{SIM} were typical of the water mass within the Prydz Bay. The difference between the two water masses can be explained by the effect of water residence time.

Deflection in the butterfly-like image was evident in the spatial distribution plots of F_{MW} and F_{SIM}. We suggest that the deflection may be due to the Ekman effect. As such, we believe that the isotope ^{2}H is a powerful tool in the study of water masses and circulations in high-latitude regions.

Depth profiles of F_{MW} in the Prydz Bay were fundamentally uniform. One explanation is that the residence time of the Prydz Bay water was long, while the input of glacial meltwater from ice shelf was a slower process relative to water mixing in the water column. We found that F_{SIM} within the basin decreased steadily with depth, and attributed the pattern to the combined effects of sea ice melting and saline water production. In the oceanic domain, vertical distribution patterns of F_{MW} and F_{SIM} were somewhat different from those within the basin. This is because of the occurrence of Circumpolar Deep Water at middle depth, where both F_{MW} and F_{SIM} were close to zero.

Our work has important implication for the study on mass balance of Antarctic Ice Cap. Since the ice melt input to the Prydz Bay can be deduced from the F_{MW} in this study when combined with water residence time, one can also derive the melting velocity of Antarctic Ice Cap by applying the same strategy to the whole Antarctic margins.

Acknowledgements We are indebted to Jiao Yutian, who provided us with the hydrographical data. Thanks are also due to Prof. Fu Zilang for his helpful comments pertaining to the manuscript. This work was supported by the grants to YPH from the National Natural Science Foundation of China (Grant No. 49836010) and the Chinese National Research Program of Science and Technology (Grant No. 98-927-01-05).

References

1. Bedard, P. C., Hillaire-Marcel, Page, P., ^{18}O modeling of freshwater in Baffin Bay and Canadian coastal waters, Nature, 1981, 293: 287—289.
2. Fairbanks, R. G., The origin of continental shelf and slope water in the New York Bight and Gulf of Maine: Evidence from $H_2{}^{18}O/H_2{}^{16}O$ ratio measurements, Journal of Geophysical Research, 1982, 87: 5796—5808.
3. Kipphut, G. W., Glacial meltwater input to the Alaska Coastal Current: Evidence from oxygen isotope measurements, Journal of Geophysical Research, 1990, 95: 5177—5181.
4. Schlosser, R., Bayer, R., Foldrik, A. et al., ^{18}O and helium as tracers of ice shelf water and water/ice interaction in the Weddell Sea, Journal of Geophysical Research, 1990, 95: 3253—3264.
5. Macdonald, R. W., Raton, D. W., Carmack, E. C., The freshwater budget and under-ice spreading of Mackenzie River water in the Canadian Beaufort Sea based on salinity and $^{18}O/^{16}O$ measurement in water and ice, Journal of Geophysical Research, 1995, 100: 895—919.
6. Jin, D., Zhang, Z., Analysis of hydrogen isotope in water by Zn reduction method, Acta Scientiarum Naturalium Universitatis Pekinensis (in Chinese), 1988, 24(6): 665—671.
7. Frew, R. D., Heywood, K. J., Dennis, P. F., Oxygen isotope study of water mass in the Princess Elizabeth Trough Antarctica, Marine Chemistry, 1995, 49 (2-3): 141—153.
8. Liu, G., Huang, Y., Jin, D. et al., Deuterium and ^{18}O contents and distributions in Antarctic snow, Journal of Xiamen University (Natural Science) (in Chinese), 2001, 40(3): 664—668.
9. Lenmann, M., Siegenthaler, U., Equilibrium oxygen- and hydrogen-isotope fractionation between ice and water, Journal of Glaciology, 1991, 37: 23—26.
10. Smith, N. R., Dong, Z., Kerry, K. R. et al., Water masses and circulation in the region of Prydz Bay, Antarctica, Deep-Sea Research, 1984, 31: 1121—1147.
11. Middleton, J. H., Humphries, S. E., Thermohaline structure and mixing in the region of Prydz Bay, Antarctica, Deep-Sea Research, 1989, 36: 1255—1266.